

# Isotropic energy and luminosity correlations with spectral peak energy for five long Gamma-Ray Bursts

Feraol F. Dirirsa<sup>1,\*</sup> and Soebur Razzaque<sup>1</sup> on behalf of the *Fermi*-LAT Collaboration

<sup>1</sup>University of Johannesburg, Kingsway Campus, Auckland Park 2006, Johannesburg

E-mail: \*fdirirsa@uj.ac.za

**Abstract.** We present a time-integrated spectral analysis of five long gamma-ray bursts (GRBs) with identified redshift and which triggered the *Fermi* satellite in 2015. Two bursts (GRB 150403A & GRB 150314A) are detected both by the *Fermi* Large Area Telescope (LAT) and Gamma-Ray Burst Monitor (GBM) while the other three sources (GRB 150727A, GRB 151027A & GRB 150301B) are detected only by the GBM. We describe the observable correlations of these bursts such as the intrinsic peak energy with the isotropic-radiated energy and luminosity in the source frame, to show their consistency with the global Amati/Yonetoku relation. We investigate the possibility that Band function, Power law (PL), Smoothly broken power law (SBPL) and Comptonized components may be present separately by fitting the prompt emission spectra in the keV-MeV energy range. At last, the intrinsic peak energy which is highly correlated to both the radiated isotropic energy (the Amati relation) and the peak luminosity (the Yonetoku relation) in the source frame is summarized.

## 1. Introduction

Gamma-ray bursts mostly emit radiation in the gamma rays which last for up to hundreds of seconds. Gamma radiation is tailed by the X-ray, optical and radio emission which last for a few days. Those bursts are the most luminous electromagnetic explosions in the Universe [1], with the highest isotropic equivalent radiated energy  $E_{iso}$ , up to  $10^{54}$  erg [2]. For the long GRBs (duration of bursts  $> 2$  s), observational correlations exist among the spectral peak energy  $E_{peak}^i$  of the prompt emission and its isotropic peak luminosity  $L_{iso}$  (so-called Yonetoku relation [3]) and isotropic radiated energy which was discovered by Amati et al. [4]. The key properties of GRBs prompt emission obtained from the time-integrated spectra of bursts with known redshift are still poorly understood. After measuring the redshift of GRB, one can correct for cosmological effects and infer its rest frame photon peak energy,  $E_{peak}^i$  of the  $\nu F_\nu$  prompt spectrum. An open issue is that if these relations have a physical origin or they are due to instrumental selection effects (or biases) which were argued by many authors [5, 6, 7]. The investigation of GRB phenomenology with spectral energy correlations have relevant implications, both for the theoretical understanding of the prompt emission and for using GRBs as standard candles in cosmological studies.

In this work, we discussed the  $E_{iso}$  and  $L_{iso}$  correlations with  $E_{peak}^i$  for five long GRBs with identified redshift  $z$  detected by *Fermi* in 2015 (*Fermi*-2015). Our analysis is based on GRB time-integrated spectra. Since, the spectra of GRBs are in a wide energy range, it can usually be described by the Band function [8], which is a smoothly broken power law with a break

energy. Below the breaking energy, the Band function reduces to a cut-off power law, while above the break energy, it is a simple power law. For the photon emission that covers large energy range, their spectra can be modelled by using a power law with exponential high-energy cut-off (Comptonized) or SBPL photon model. Using the parameters obtained from the best fit photon model, we have computed the  $E_{peak}^i$ ,  $E_{iso}$  and  $L_{iso}$  to study the Amati relation ( $E_{peak}^i$  -  $E_{iso}$ ) and Yonetoku relation ( $E_{peak}^i$  -  $E_{iso}$ ). For the two *Fermi* LAT/GBM detected GRBs (GRB 150403A & GRB 150314A), we considered unbinned likelihood analysis using the pass 8 data [9] to determine the probability of photons coming from each event. Throughout the paper, we assume a flat-isotropic universe with  $H_0 = 69.6 \text{ km s}^{-1} \text{ Mpc}^{-1}$ ,  $\Omega_\Lambda = 0.714$  and  $\Omega_m = 0.286$ . Calculations of luminosity distances are done using the analytical approximation [10].

## 2. Sample and method of data analysis

We considered the GRBs detected by the *Fermi* satellite in 2015 with known redshift. In our sample, there are 5 long GRBs (observed duration  $> 2 \text{ s}$ ). Among these bursts, GRB 150403A & GRB 150314A are simultaneously detected by both LAT and GBM while the other three sources GRB 150727A, GRB151027A & GRB 150301B are triggered only by GBM as shown in Table 1. To analysis the LAT-detected GRBs with known redshift, we have selected the high energy data between 0.1 GeV and 30 GeV. The highest-energy ( $E_{max}$ ) photon of the GRB 150314A is a  $\sim 0.62$  GeV photon (with 97.8 % probability of being associated with GRB) and for the GRB 150403A, it is  $\sim 5.4$  GeV (with 99.6 % probability) which are observed at  $\sim 81$  s and  $\sim 632$  s after the GBM trigger, respectively. The GBM light curve of both GRB 150314A and GRB 150403A shows a bright single pulse with a duration  $T_{90}$  [11] of about 10.7 s and 22.3 s with energy range computed between 50 and 300 keV, respectively. The GBM light curve of GRB 150301B consists of one main peak, the GRB 150727A light curve shows a FRED-like (fast-rise exponential-decay) pulse and the GRB 151027A light curve consists of three pulses with a duration  $T_{90}$  of about 13 s, 50 s, and 124 s, respectively as shown in Table 1.

**Table 1.** Data on *Fermi* LAT/GBM detected GRBs with known redshift.

GRB	z	$T_{90}(\text{s})^f$	Best on-ground location	# of HE photons <sup>l</sup>	Detectors
150314A	1.758 <sup>a</sup>	10.7	(RA, Dec)=125.40, 64.46 <sup>g</sup>	9	<i>Fermi</i> -LAT/GBM
150403A	2.06 <sup>b</sup>	22.3	(RA, Dec)=311.79, -62.76 <sup>h</sup>	6	<i>Fermi</i> -LAT/GBM
150301B	1.517 <sup>c</sup>	13	(RA, Dec)=89.157, -57.977 <sup>i</sup>	-	<i>Fermi</i> -GBM
150727A	0.313 <sup>d</sup>	50	(RA, Dec)=203.99, -18.355 <sup>j</sup>	-	<i>Fermi</i> -GBM
151027A	0.81 <sup>e</sup>	124	(RA, Dec)=272.491, 61.381 <sup>k</sup>	-	<i>Fermi</i> -GBM

<sup>a</sup>de Ugarte Postigo A., et al., 2015, (GCN 17583)    <sup>g</sup>Axelsson M., et al., 2015, (GCN 17576)  
<sup>b</sup>Pugliese V., et al., 2015, (GCN 17672)    <sup>h</sup>Longo F., et al., 2015, (GCN 17667)  
<sup>c</sup>Lien Y., et al., 2015, (GCN 17515)    <sup>i</sup>de Ugarte Postigo A., et al., 2015, (GCN 17523)  
<sup>d</sup>Watson M., et al., 2015, (GCN 18089)    <sup>j</sup>Cenko B., et al., 2015, (GCN 18076)  
<sup>e</sup>Perley A., et al., 2015, (GCN 18487)    <sup>k</sup>Maselli A., et al., 2015, (GCN 18478)  
<sup>f</sup>The time between accumulating 5% & 95% of the counts associated with the GRB    <sup>l</sup>The number of High Energy (HE) photons with probability  $> 90\%$

### 2.1. Spectral analysis

For the time-integrated spectral analysis, data from the optimal sodium iodide (NaI) detectors were fitted together with bismuth germanate (BGO) detectors [12]. As in most of the previous spectral analysis of GRBs, we used SBPL, Power law function with an exponential high-energy cutoff [Comptonized (Comp)], Band function (Band) [8] and PL models. For the triggers

selection, the criterion adopted in Guiriec et al. [13] is implemented. To perform the spectral analysis, the recently released software RMFIT (*v3.3pr7*) [14] tool kits has been used. The NaI data from  $\sim 10$  keV to  $\sim 915$  keV and the BGO data from  $\sim 250$  keV to  $\sim 10$  MeV are used by cutting out the overflowing low and high-energy channels as well as the K-edge from  $\sim 30$  to  $\sim 40$  keV. The background in each of the GBM detectors was estimated by fitting polynomial functions to the light curves in various energy ranges before and after the source active time period. For GBM data, the background was fitted to the CSPEC data which cover a much longer time range, making the estimation of the background more reliable for long GRBs [15]. For GRB 151027A, GRB 150727A, GRB 150403A, GRB 150314A and GRB 150301B, the triggers (n0+n1+n3+b0), (n0+n3+n4+b0), (n3+n4+b0), (n0+n1+n2+n9+na+b0) and (n0+n3+n4+n6+n7+n8+b0+b1) are used for the time-integral analysis for the time section  $T_{90}$  [11] and  $T_{peak}$  (the time at high peak count rate), respectively.

### 3. Data analysis

The spectral parameters in Tables 2 and 3 have been obtained through the analysis of the time-integrated spectrum extracted from the GBM data by performing the software package RMFIT for the duration of  $T_{90}$  and  $T_{peak}$  in the  $\sim 10$  keV to  $\sim 10$  MeV energy range, respectively. The best spectral parameter values were estimated by optimizing the Castor C-statistic (hereafter C-stat), which is a likelihood technique that converges to  $\chi^2$  for a specific data set when there are enough counts. We have selected the best model by choosing the fit with the lowest C-stat value after each of the spectrum fitted with a Band, PL, SBPL and Comp models. Tables 2 and 3 show the results of these fits. Table 2 lists 5 long GRBs with their time integrated spectral parameters (columns 3, 4, and 7) and the time integrated isotropic radiated energy, computed in the rest frame in the 1 keV - 10 MeV energy range ( $L_{iso}$ , Column 5) and derived intrinsic peak-energy ( $E_{peak}^i$ , Column 6). Table 3 contains, the spectral analysis of five long GRBs for  $T_{peak}$  with the obtained parameters (columns 3, 4, and 5) and derived intrinsic peak luminosity, computed in the rest frame in the 1 keV - 10 MeV energy range ( $L_{iso}$ , column 6). Figures 1 and 2 show the Band spectrum fit of GBM data of GRB 150403A & GRB 150314A,

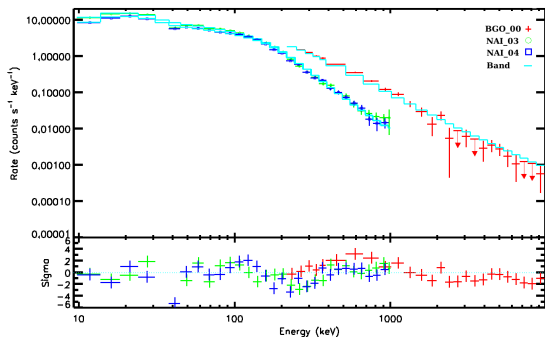


**Figure 1.** The time-integrated spectrum of GRB 150403A fitted by a Band function.

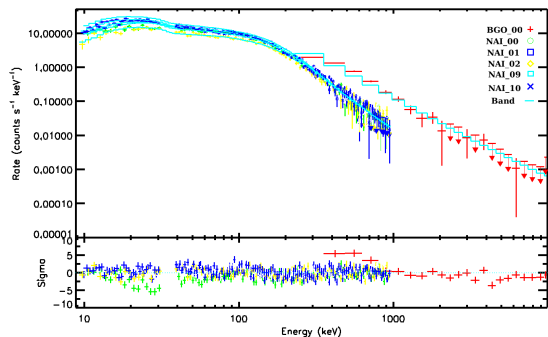


**Figure 2.** The time-integrated spectrum of GRB 150314A fitted by a Band function.

respectively. These bursts are detected by both the LAT and GBM. As shown in Tables 2 and 3, the GRB 150403A and GRB 150314A show a high band model component and their observed peak energies are the largest of the sample. In tables 2 & 3, the associated errors reported on  $E_{iso}$ ,  $L_{iso}$  and  $E_{peak}^i$  was computed by properly weighing for data uncertainties [16] except for GRB 150314A, we assume 10% error in these measurements due to some statistical errors on the parameters.

**Table 2.** Results of the spectral fits for the duration of  $T_{90}$  and derived  $E_{iso}$  in the GRB rest frame.

GRB	$T_{90}$ [sec.]	$\alpha$ /Index1	$\beta$ /Index2	$E_{iso}/10^{52}$ [erg]	$E_{peak}^i$ [keV]	$E_{peak}$ [keV]	Model	C-stat/dof
151027A	-2.048 - 133.120	-1.47 ± 0.039	-	2.99 ± 0.365	592.6 ± 112.9	327.4 ± 62.4	Comp	866.55/430
		-1.46 ± 0.06	-1.98 ± 0.12	-	-	-	SBPL	863.56/429
		-1.66 ± 0.02	-	-	-	-	PL	908.54/431
150727A	0.003 - 50.177	-0.38 ± 0.20	-2.18 ± 0.21	0.32 ± 0.14	224.3 ± 37.7	170.8 ± 27.2	Band	1060.0/424
		-0.59 ± 0.12	-	-	-	220.8 ± 19.5	Comp	1066.6/425
		-0.58 ± 0.2	-2.19 ± 0.19	-	-	-	SBPL	1060.3/424
		-1.48 ± 0.02	-	-	-	-	PL	1191.3/426
150403A	-0.512 - 23.04	-0.77 ± 0.02	-2.04 ± 0.04	93.52 ± 4.46	1172.6 ± 43.1	383.2 ± 14.1	Band	438.65/315
		-0.88 ± 0.01	-	-	-	531.3 ± 13.4	Comp	550.79/316
		-0.87 ± 0.02	-1.99 ± 0.03	-	-	-	SBPL	434.55/315
		-1.37 ± 0.004	-	-	-	-	PL	4113.5/317
150314A	-2.912 - 11.424	-0.58 ± 0.01	-2.35 ± 0.04	87.4 ± 8.74	870.7 ± 87.1	315.7 ± 5.2	Band	1354.2/660
		-0.65 ± 0.008	-	-	-	367.6 ± 4.2	Comp	1467.6/661
		-0.73 ± 0.009	-2.25 ± 0.03	-	-	-	SBPL	1359.3/660
		-1.34 ± 0.003	-	-	-	-	PL	15663/662
150301B	-2.56 - 13.824	-1.13 ± 0.09	-2.21±0.25	3.64 ± 0.97	498.85 ± 98.16	198.2 ± 39.0	Band	963.3/857
		-1.19 ± 0.06	-	-	-	244.3 ± 30.1	Comp	965.44/858
		-1.28 ± 0.06	-2.35± 0.29	-	-	-	SBPL	963.45/857
		-1.60 ± 0.02	-	-	-	-	PL	1043.3/859

**Table 3.** Results of the spectral fits for the duration of  $T_{peak}$  and  $L_{iso}$  in the GRB rest frame.

GRB	$T_{peak}$ [sec.]	$\alpha$	$\beta$	$E_{peak}$ [keV]	$L_{iso}$ [erg/s]	Model	C-stat/dof
151027A	0.002 - 1.792	-0.71 ± 0.096	-2.28 ± 0.19	170.0 ± 19.9	0.36 ± 0.096	Band	439.14429
		-0.83 ± 0.06	-	208.7 ± 14.7	-	Comp	448.7/430
		-0.96 ± 0.07	-2.46 ± 0.23	-	-	SBPL	439.06/429
		-1.52 ± 0.02	-	-	-	PL	664.73/431
150727A	4.096 - 6.144	-0.59 ± 0.31	-3.13 ± 3.58	273.3 ± 89.4	-	Band	402.16/426
		-0.58 ± 0.28	-	273.9 ± 65.2	0.0101 ± 0.0053	Comp	402.24/427
		-0.89 ± 0.21	-4.35 ± 5.42	-	-	SBPL	402.46/426
		-1.42 ± 0.056	-	-	-	PL	420.79/428
150403A	10.752 - 12.80	-0.66 ± 0.03	-2.14 ± 0.06	480.0 ± 26.4	20.55 ± 1.55	Band	338.08/294
		-0.79 ± 0.02	-	649.6 ± 24.6	-	Comp	424.79/295
		-0.77 ± 0.032	-2.08 ± 0.05	-	-	SBPL	339.86/294
		-1.38 ± 0.008	-	-	-	PL	1688.0/296
150314A	1.184 - 3.232	-0.296 ± 0.018	-2.4 ± 0.048	293.6 ± 5.6	22.2 ± 2.22	Band	1041.0/656
		-0.42 ± 0.01	-	352.3 ± 4.48	-	Comp	1159.7/657
		-0.49 ± 0.02	-2.32 ± 0.04	-	-	SBPL	1061.6/657
		-1.31 ± 0.004	-	-	-	PL	11083/658
150301B	1.536 - 3.584	-1.07 ± 0.12	-2.39 ± 0.53	211.7 ± 50.4	0.55 ± 0.203	Band	933.9/856
		-1.13 ± 0.09	-	249.4 ± 40.5	-	Comp	934.2/857
		-1.21 ± 0.098	-2.34 ± 0.37	-	-	SBPL	934.53/856
		-1.59 ± 0.03	-	-	-	PL	987.46/858

## 4. Correlation

### 4.1. Amati relation

In order to determine the strength and significance of  $E_{peak}^i$  -  $E_{iso}$  correlation, we utilized a linear regression analysis using the Pearson's and Spearman's correlation. For this purpose we undertake a comparison between the Amati relation of the *Fermi*-2015 data analysis and the sample populations of 68 GRBs from Amati et al, 2008 (A2008) [17]. These data are shown in Figure 3. The computation of  $E_{iso}$  was determined in the rest-frame from 1 keV to 10 MeV energy range and the  $E_{peak}^i = E_{peak}(1+z)$ . The black dashed line is the best-fit power law that obtained by weighting each point by its error on both  $E_{peak}^i$  and  $E_{iso}$  for 5 *Fermi*-2015 GRBs.

The power law fit gives  $E_{peak}^i[\text{keV}] = (338.6 \pm 78.0) (E_{iso}/10^{52}\text{erg})^{0.26 \pm 0.053}$  with the reduced  $\chi_{red}^2 = 3.14$ . The Spearman's rank correlation coefficient proved a high correlation value of  $\rho_{sp} = 0.9$  with the chance probability  $P_{sp} = 0.037$ . Also, the Pearson's coefficient for this correlation is  $\rho_p = 0.70$  with an extremely low value of the chance probability  $4.34 \times 10^{-12}$ . The combination of *Fermi*-2015 and A2008 data are also fitted together by power law. The best fit power law shown by magenta solid line results  $E_{peak}^i[\text{keV}] = (93.1 \pm 6.23) (E_{iso}/10^{52}\text{erg})^{0.56 \pm 0.02}$  with the reduced  $\chi_{red}^2 = 6.69$ .

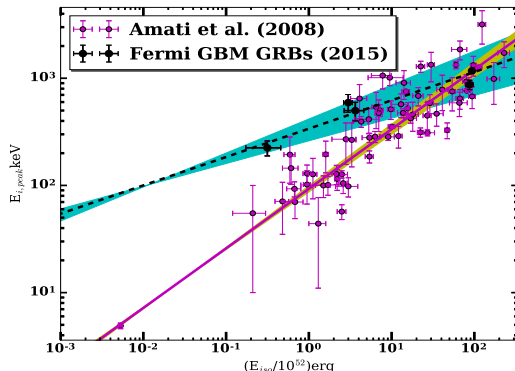


**Figure 3.** The  $E_{peak}^i$  -  $E_{iso}$  relation. The black circles are our present results of five long *Fermi* GRBs. The data from A2008 [17] are shown by the magenta circles. Both results are plotted as  $E_{peak}^i$  at the rest frame of the GRBs and the  $E_{iso}$  is calculated using the  $T_{90}$  fluence.

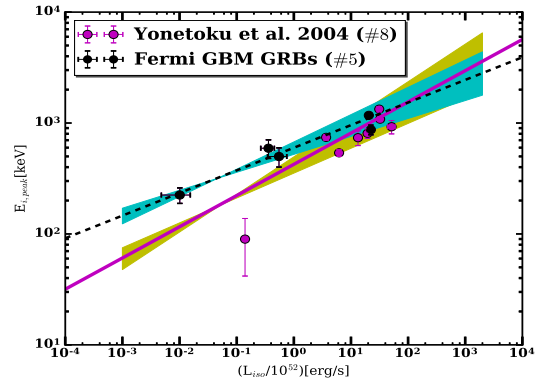


**Figure 4.** The  $E_{peak}^i$  -  $L_{iso}$  relation. The black circles are our present results with five *Fermi* GRBs. The results of Yonetoku et al., 2004 (Y2004) [3] is also shown as the magenta circles. Both results are plotted as  $E_{peak}^i$  at the rest frame of the GRBs and the peak luminosity derived from the time  $T_{peak}$  flux.

#### 4.2. Yonetoku relation

Another correlation among observable quantities is between  $E_{peak}^i$  and  $L_{iso}$  (Yonetoku correlation). In this correlation analysis, we computed the  $L_{iso}$  emitted at the 1-second peak of the light curve from 1 keV to 10 MeV band. In Figure 4, we have shown the plots of the peak luminosity as a function of intrinsic peak energy for both the data of *Fermi*-2015 GRBs and its combination with 8 GRBs in Yonetoku et al. 2004 (Y2004) [3]. In Y2004 data, the redshift of GRB 980326 and GRB 980329 are not precisely determined and only the upper limit of intrinsic peak energy has been reported for GRB 980703. Therefore, we can exclude these three bursts from our data analysis to avoid inaccurate result. When we adopt the power-law model to the  $E_{peak}^i$  -  $L_{iso}$  relation, the best-fit function (magenta solid line) of 5 *Fermi*-2015 data is  $E_{peak}^i[\text{keV}] = (598.4 \pm 76.9) (L_{iso}/10^{52}\text{ergs}^{-1})^{0.20 \pm 0.04}$  with the reduced  $\chi_{red}^2 = 3.66$ . The Spearman's rank correlation coefficient is 0.8 with chance probability 0.104. The best power-law fit (magenta solid line) for the *Fermi*-2015 data (black circles) together with Y2004 data (magenta circles) is  $E_{peak}^i[\text{keV}] = (424.2 \pm 70.96) (L_{iso}/10^{52}\text{ergs}^{-1})^{0.28 \pm 0.06}$  with the reduced  $\chi_{red}^2 = 8.3$ . The Pearson's correlation coefficient is  $\rho_p = 0.74$  with the chance probability  $P_p = 0.0036$ . The Spearman's rank correlation coefficient also gives  $\rho_{sp} = 0.89$  with the chance probability  $P_{sp} = 4.565 \times 10^{-5}$ .

## 5. Discussion

We studied the time-integrated spectra of five *Fermi* GRBs by fitting time-integrated spectra over the duration of  $T_{90}$  and  $T_{peak}$  in the  $\sim$ 10 keV -  $\sim$ 10 MeV energy range, respectively. The spectral parameters obtained from this analysis are reported in Tables 2 and 3, where the Band function considered as adequately fitting GRB spectra. For the *Fermi*-2015 GRB observables, we found a high correlation of peak energy with isotropic radiated energy and the peak luminosity in the GRB source frame. For the *Fermi*-2015 data, there is a higher and tighter correlation between  $E_{peak}^i$  and  $E_{iso}$ . Their best-fit power law index is  $0.26 \pm 0.053$  with the reduced  $\chi^2_{red} = 3.14$ . This looks considerably tighter and more reliable than the relations suggested by the previous works [18, 19]. The best-fit power law index for the *Fermi*-2015 and A2008 joint data is  $0.56 \pm 0.02$  with the reduced  $\chi^2_{red} = 6.69$ , which has a similar result with the previous Amati [17] correlation (i.e. the index of the power-law  $\sim 0.57$  and  $\chi^2_{red} = 7.2$ ). The Spearman's rank correlation coefficient also shows a high correlation between the observables  $E_{peak}^i$  and  $E_{iso}$  ( $\rho_{sp} = 0.9$ ). As shown in Fig. 4, the *Fermi*-2015 and Y2004 data are poorly fitted by the power low with reduced  $\chi^2_{red} = 8.3$ . This indicates that the fit has not fully captured the relationship between the observable. However, the Pearson's correlation coefficient ( $\rho_p = 0.74$ ) and the Spearman's rank correlation coefficient ( $\rho_{sp} = 0.89$ ) are indicating a positive strong correlation. For the  $L_{iso}$  -  $E_{peak}^i$  correlation analysis, our results are limited by the small number of GRBs in the sample (i.e., 13 GRBs). To get a more reliable conclusion, the number of GRBs with well-determined redshifts and spectra needs to be significantly expanded.

## Acknowledgments

The *Fermi*-LAT Collaboration acknowledges support for LAT development, operation and data analysis from NASA and DOE (United States), CEA/Irfu and IN2P3/CNRS (France), ASI and INFN (Italy), MEXT, KEK, and JAXA (Japan), and the K.A. Wallenberg Foundation, the Swedish Research Council and the National Space Board (Sweden). Science analysis support in the operations phase from INAF (Italy) and CNES (France) is also gratefully acknowledged. The work presented in this paper was supported in part by an MWGR 2015 grant from the National Research Foundation with Grant No. 93273.

## References

- [1] Piran T 1999 *Phys.Rept.* **314** 575
- [2] Amati L 2006 *MNRAS* **372** 233
- [3] Yonetoku D *et al.* 2004 *ApJ* **609** 935
- [4] Amati L *et al.* 2002 *A&A* **390** 81
- [5] Heussaff V, Atteia J L and Zolnierowski Y 2013 *A&A* **557** A100
- [6] Ghirlanda G *et al.* 2012 *MNRAS* **422** 2553
- [7] Nava L, Ghirlanda G and Ghisellini G 2009 *arXiv preprint arXiv:0902.1522*
- [8] Band D *et al.* 1993 *ApJ* **413** 281
- [9] Atwood W *et al.* 2013 *ApJ* **774** 76
- [10] Wright E L 2006 *ASP* **118** 1711
- [11] Ackermann M *et al.* 2010 *ApJ* **716** 2
- [12] Meegan C *et al.* 2009 *ApJ* **702** 791
- [13] Guiriec S *et al.* 2010 *ApJ* **727** L33
- [14] <http://fermi.gsfc.nasa.gov/ssc/data/analysis/rmf/>
- [15] Guiriec S *et al.* 2015 *ApJ* **807** 148
- [16] Bevington J 1969 *McGrawHill* 36
- [17] Amati L *et al.* 2008 *ApJ* **390** 81
- [18] Dirirsa F F and Razzaque S 2015 *PoS(SSC2015)066*
- [19] Amati L 2005 *MNRAS* **372** 233